Computational and Theoretical Chemistry 1095 (2016) 112–117

Contents lists available at ScienceDirect

Computational and Theoretical Chemistry

journal homepage: www.elsevier.com/locate/comptc

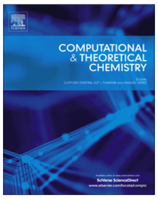

Electronic properties of $SrFeO_2$ doped by Ca and Ba: A first-principles study

Miao Jiang, Naihang Deng, Yongqing Qiu *

Institute of Functional Material Chemistry, Faculty of Chemistry, Northeast Normal University, Changchun 130024, People's Republic of China

ARTICLE INFO

Article history:
Received 15 July 2016
Received in revised form 20 September 2016
Accepted 20 September 2016
Available online 21 September 2016

Keywords:
First-principle calculations
Perovskite
Doping
Electronic conductivity

ABSTRACT

ABO_2-type perovskite materials have been wide applied in solid oxide fuel cells and gas sensors. $SrFeO_2$ with $P4/mmm$ structure exhibiting an unparalleled FeO_4 square-planar coordination structure. We have investigated the Sr-site substitution effect on the electronic conductivity of the perovskite-type structure of $(Sr_{1-x}Ca_x)FeO_2$ and $(Sr_{1-x}Ba_x)FeO_2$ (x = 0, 0.25, 0.5, 0.75) by using first-principle calculations. Six kinds of doping form have been considered for the Ca-site and Ba-site, respectively. The different doping concentration and position lead to change in crystal structure and electronic properties. When x = 0.5, α and β doping structures display $Pmmm$ symmetry, while γ and δ doping structures show $P4/mmm$ symmetry. The band structure and density of states reveal that different doping concentration and position can make the electronic conductivity change from semiconductor to semi-metallic. When x = 0.25, 0.75, 0.5 for γ and δ doping, the doped system were semi-metallic properties. Whereas, when x = 0.5 for α and β doping, the doped system were semiconductor properties. Further, doping can lead to an increase of the magnetic moments. It is worth noting that the Ca-doped system has higher growth in the magnetic moments compare with the Ba-doped system. This work provides a new route for the potential application in electrochemistry devices.

1. Introduction

ABO_3 as the high stability of the perovskite structure allows the substitution of A and B sites for various elements (A = rare-earth, alkali or alkaline earth metal, B = transition metal) [1–5], the material are used in application that include gas sensors [4,6], magnetic coupling [7,8], exhaust gas CO [9,10] and NO_x treatment [11,12]. However, the perovskite-type ($AFeO_{3-\delta}$) ($0 \leqslant \delta \leqslant 1$) structures have attached much attention because of their special properties and offer a promising candidate for the oxygen vacancy [3,5,13–15], especially for ABO_2, which displays a new sight into the infinite-layer (IL) structure [13,16,17]. Recently, Tsujimoto et al. reported a novel synthesized compound $SrFeO_2$, consisted of two-dimensional FeO_2 layers with each Fe atom sharing strongly FeO_4 squares separated by Sr^{2+} [13,18–23]. The structure always preserved the square planar during the A site substitution [24]. Fe atoms in the perovskite have the valance state of −2. The novel structure of $SrFeO_2$ are three-dimensionally (3D) ordered, belonging to $P4/mmm$ space group with the parameter of $a = b = 3.985$ Å and $c = 3.458$ Å [13,25]. Under the ambient condition, $SrFeO_2$ has the three-dimensional ($\pi\pi\pi$) antiferromagnetic property [25–27]. $SrFeO_2$ shows a remarkable stability to tolerate distortion to adapt different A site substitution [28]. The perovskite-type structure of $(Sr_{1-x}A_x)FeO_2$ has gained extensive studies for many years due to that the doping can optimize the crystal structures and ionic conductivity of materials [3]. Since the discovery of $SrFeO_2$ and $(Sr_{1-x}A_x)FeO_2$, the materials have gained extensive applied in industry such as gas sensors [18] and electrodes for solid oxide fuel cells [3,29].

There are numerous studies on the use of ABO_2-type perovskite; most A and B of these materials are substituted by other cation. It's well-known that substitution can cause the electronic conductivity change. For A site substitution, such as $(Ba_{1-x}La_x)FeO_{3-\delta}$ ($\delta = 0.125$, 0.25, 0.375), when x = 0.125 with the increasing of oxygen deficiencies lead to transition from semi-metallic to *p*-type semiconductivity and finally show semi-metallic properties [3]. For $(La_{1-x}Sr_x)FeO_{3-\delta}$ ($0 \leqslant x \leqslant 0.75$), with the increasing of Sr site substitution concentration, the crystal structure transform from orthorhombic, via rhombohedral to cubic and display the semiconductor properties for $x \leqslant 0.5$ [14,30]. For B site substitution, such as $Sr(Fe_{1-x}B_x)O_2$ (B = Mn, Co), when $x \leqslant 0.3$ show the insulator properties and retaining the infinite layer structure with $P4/mmm$ space symmetry [19,27,31]. For $(Sr_{1-x}Ca_x)FeO_2$, the FeO_4 maintain the square planar for $0 \leqslant x \leqslant 0.8$ and when x = 1 for $CaFeO_2$, the FeO_4

---

* Corresponding author.
E-mail address: qiuyq466@nenu.edu.cn (Y. Qiu).

http://dx.doi.org/10.1016/j.comptc.2016.09.025

units distort from square-planar to tetrahedra and eventually form the infinite FeO_2 units (space group $P\text{-}42_1m$) [23]. For $(Sr_{1-x}Ba_x)FeO_2$, the FeO_4 remain the square planar for $0 \leqslant x \leqslant 0.3$ and $x = 1$ for $BaFeO_2$ have $P4/mmm$ tetragonal symmetry, which is similar with $SrFeO_2$ [24,32,33]. The doped crystal structure of $(Sr_{1-x}Ca_x)FeO_2$ and $(Sr_{1-x}Ba_x)FeO_2$ has been observed, but the electronic conductivity has not been investigated. Thus the investigation of A and B site substitution for $SrFeO_2$ also represents forward to understanding the electronic conductivity property.

In this work, we calculated the Ca-substitution and Ba-substitution effect on the crystal structure and electronic conductivity of novel perovskite structure of $SrFeO_2$ based on the first-principles density functional calculations. When x = 0.5, exist of two kinds of structures. The band structure and density of states reveal that doping can lead to the electronic conductivity change from semi-conductor to semi-metallic and we find that doping can increase the magnetic moments.

2. Computational method

The structural optimization and electronic properties calculation were calculated by density functional theory (DFT) method with a plane-wave basis set, as implement in Vienna *ab initio* Simulation Package (VASP) [21,34–40]. We used the projected augmented waves (PAW) with the generalized gradient approximation (GGA) [4,20,26] plus the effective Coulomb repulsion parameter U_{eff} for Fe ($U_{eff} = 5$). The electron-ion interaction was described by projected-augmented-wave potentials with $2p^6$, $3d^6$, $4s^2$, $5s^2$, $6s^2$ and as valance electrons for O, Fe, Ca, Sr and Ba, respectively. The use of the plane-wave cutoff is set to 400 eV and Brillouin-zone (BZ) is set to $4 \times 4 \times 4$ Monkhorst-Pack grid. The electronic energy tolerance is set to 10^{-6} and the force tolerance for the structural relaxation is 0.001 eV/Å. The crystal structures were explained by using the VESTA program [41].

3. Results and discussion

The optimized lattice parameters are $a = b = 4.012$ Å, $c = 3.427$ Å and the magnetic moment is 3.9 μB, which are in highly agreement with the experimental values of $a = b = 3.985$ Å, $c = 3.458$ Å [13] and the experimental magnetic moment is 3.6 μB [17], respectively, validating our methodology in application to this system. The perovskite $2 \times 2 \times 2$ super-cell with 32 atoms of $SrFeO_2$ were chosen to as A site substitution structure (Fig. 1b) and the different doping concentration is shown in Fig. 1c–h. To address the role of Ca site substitution, we considered six kinds of arrangements of Sr and Ca within the Sr sublattice (Fig. 1c–h). For Ca-doped system, when concentration up to x = 0.25 and x = 0.75, we only consider one kind of doping position as displayed in c and d, respectively; when x = 0.5, we consider four kinds of arrangement for the composition to investigate the effect on electronic conductivity, the unique arrangement for x = 0.5 is shown in Fig. 1e–h, namely α, β, γ and δ. When x = 0.5, four Ca atoms of α and β structure substitute Sr at the parallel position; four Sr atoms of γ and δ structure are replaced by Ca at the diagonal position. For Ba-doped system, we consider the same doping concentration and occupation as Ca-doped system (Fig. S1(a)–(f)). The fully relaxed crystal structure of Ca-doped and Ba-doped system were shown in Figs. 1(i)–(l) and S1(g)–(j). It's a notable finding that when x = 0.5 for Ca-doped and Ba-doped structure, the γ and δ structure doping display $P4/mmm$ symmetry (Fig. 1k and l), which is similar with $SrFeO_2$ (Fig. 1a), however for α and β structure doping show $Pmmm$ symmetry (Fig. 1i and j). As seen in Table 1, for α and β structure there has larger Fe-O bond lengths compare to γ and δ structure, so α and β has weaker Fe-O interactions than γ and δ structure. There are two kinds of space group $P4/mmm$ and $Pmmm$ in different doping position, indicating that the doping position have effect on crystal structure. In order to explain the problem of site substitution, our key observation is the followings.

The different of A site substitution in $SrFeO_2$, a different electronic effect for each site doping is expected. To understand the electronic conductivity of Sr site substitution, we calculated the spin-polarization of the electronic band structure and density of states (DOS) for Ca and Ba substitution were shown in Figs. 2, 3 and S2–S5, respectively. The band gaps of doping are presented in Table 1. For Ca-doped system, when x = 0.25 and 0.75 the energy band cross the Fermi level for spin-up and the band gap is 1.31 eV, 1.26 eV for spin-down, respectively, indicating the semi-metallic properties (Fig. 2a and b); for Ba-doped system, the energy band cross the Fermi level for spin-up and the band gap is 1.32 eV and 1.07 eV for spin-down, respectively, also indicating the semi-metallic properties (Fig. 3a and b). When x = 0.5, for Ca-doped system, the α structure of band gap is 0.9 eV and 1.65 eV for spin-up and spin-down, respectively, indicating the semiconductor properties (Fig. 2c); for Ba-doped system, the α structure of band gap is 0.58 eV and 1.79 eV for spin-up and spin-down, respectively, also indicating the semiconductor properties (Fig. 3c). For α structure doping, the band gap for spin-up and spin-down are both smaller than $SrFeO_2$ (2.33 eV and 2.63 eV for spin-up and spin-down, respectively); however, for γ structure doping, the Ca-doped (Ba-doped) structure of energy band cross the Fermi level for spin-up and the band gap is 1.28 eV (1.26 eV) for spin-down, indicating the semi-metallic properties (Figs. 2d and 3d). It is interesting to find that when concentration up to x = 0.5, we consider four kinds of site occupation, and obtain two results for site different occupation position: α and β has the semiconductor properties, γ and δ shows the semi-metallic properties, respectively. As above mentioned data, there is the same doping concentration, the different doping occupation influences the electronic conductivity.

We calculated the energy gap of Ca-doped and Ba-doped $SrFeO_2$. As can be seen from Table 1, $SrFeO_2$ has an energy gap of 0.98 eV, which is in agreement with previously theoretical reported (1.1 eV) [33]. For Ca-doped system, the doping of Ca atom makes the energy gap increases than $SrFeO_2$. At the same time, the energy gap increase with the Ca-doped concentration increase, the energy gap of α and β structure larger than γ and δ structure, indicating that γ and δ structure has better electronic conductivity compare to α and β structure, which is in consistent with stronger Fe—O interactions in γ and δ structures; for Ba-doped system, the doping of Ba atom makes the energy gap increases than $SrFeO_2$. At the same time, the energy gap decreases with increasing of the Ba-doped concentration and energy gap of α and β structure larger than γ and δ structure, indicating that γ and δ structure has better electronic conductivity compare to α and β structure, which is in consistent with stronger Fe—O interactions in γ and δ structures. Although doping of Ca and Ba atom belong to the same group in the periodic table of elements (IIA), they have different effects for electronic conductivity in varies doping. There was reported that Pt doping induce the mid-gap that shifts the Fermi level [42], however in our work, the Ca-doped and Ba-doped system haven't induce mid-gap states, which is similar with theoretical reported [43]. From the DOS of Ca-doped and Ba-doped system as were shown in Figs. 2 and 3 and S2–S5, there has a common feature for the doping compounds: both valance band and conduction band are mainly O 2*p* in character, while doping of Ca and Ba atom minority contributes to the total DOS. Moreover, the DOS is asymmetry at the Fermi level, which shows the magnetism of Ca-doped and Ba-doped system. With the increasing of site doping concentration, the magnetic moments were shown in Table 1. We can see that Ca-doped system has larger magnetic moment compare to Ba-doped system. The phenomenon can be explained by with